ISSN : 0974 - 7435 Volume 11 Issue 8

BioTechnology
An Indian Journal

FULL PAPER

BTAIJ, 11(8), 2015 [311-319]

Oxidation stability of palm oil methyl ester (POME) as biodieseland its corrosiveness behavior

A.M.Muzathik[1,2]*, H.D.Tan[1], Khalid Samo[1], W.B.Wan Nik[1]

[1]Department of Maritime Technology, FMSM, University Malaysia Terengganu, Kuala Terengganu, Terengganu, (MALAYSIA)

[2]Department of Mechanical Engineering, Faculty of Engineering, South Eastern University of Sri Lanka, Oluvil, (SRILANKA)

E-mail : muzathik64@yahoo.com

ABSTRACT

This research was conducted to study the oxidation stability of Palm Oil Methyl Ester (POME) as biodieseland its corrosiveness behavior. Aluminiumalloy was used to study corrosiveness behavior and tested using Electrochemical Impendence Spectroscopy. Biodiesel samples were tested to define their functional group by using Fourier Transform Infrared Spectroscopy. There wereonlyslight changes in weight of test samples and there was a decreased of corrosion rate. As conclusion, POME biodiesel prohibited and resists the corrosion attack on Aluminiumdue to formation of an oxide layer.

KEYWORDS

Biodiesel;
Corrosion;
Electrochemical impendence spectroscopy (EIS);
Fourier transform infrared spectroscopy (FT-IR);
Oxidation stability;
Palm oil methyl ester (POME).

INTRODUCTION

Biodiesel, which is a new, renewable and biological origin alternative diesel fuels to substitute fossil fuel for diesel engines. The source of vegetable oil is a crop and they promote self-reliance as ample production capacity exists. But the source of mineral oil is a finite mineral deposit. Biodiesel which having the similar chemical structures as fossil fuels but non-toxic compare to diesel fuel and usually produced based on the various types of food grade vegetable oils (palm, soybean, sunflower, etc.) by using the transestrification process. Biodiesel (methyl ester of palm oil) commonly known as palm oil diesel[1-3].

Biodiesel is defined as the fatty acid alkyl monoesters derived from the plants where composed of mainly triglycerides, contains small amount of partial glycerides, free fatty acids and non-glyceride substances[4]. Biodiesel consisting of long-chain fatty acid methyl ester (FAME)which derived from the biological sources such as vegetable oil or animal fats by the transesterification of triglycerides and alcohol in the presence of a catalyst[5].

Although biodiesel has a bright future as the substitution of fossil fuel but the use of biodiesel still faces some challenges, including the problems of corrosion of fuel containers, low storage stability and oxidation stability of biodiesel[6]. Oxidative stability is the parameters that describe the degradation tendency of biodiesel and a great importance in content of possible problems with engine parts[7]. Biodiesel stability generally depends on fatty acid profile of the parent stock in result the

FULL PAPER

biodiesel with high contents of the unsaturated fatty acids such as linoleic and linolenic which are especially prone to oxidation. The relative oxidation rates fir these unsaturated esters are linolenic, linoleic and oleic[7]. Oxidation stability of vegetable oils depends on the level of unsaturated products presents. The lower the unsaturation the better oxidative stability but higher melting point[3]. The oxidation can lead to the formation of corrosive acids and deposits that may cause increased wear in engine fuel pumps[8].

When oxidation occurs at ordinary temperatures, the initial products are hydroperoxides. The presence of the acids will increase the total acidity or total acid number (TAN) and the risk of corrosion due to the further degradation of the peroxides and hydroperoxides[7]. Oxidation process is the most important reaction of oils resulting in increased acidity, corrosion, viscosity and volatility when used as lubricant based oils[9]. Oxidative stability depends on the presence of unsaturated fatty acids in the triacyglycerol molecule due to the double bond (C=C) in fatty acid. For example, the lower unsaturation the better oxidative stability but with higher pour point. Reaction of the double bond includes hydrogen abstraction, addition reaction, fragmentation, rearrangement, disproportionate reaction and polymerisation. Unsaturated fatty alkyl chains react with molecular oxygen to form free radical that lead to polymerisation and fragmentation[8].

Biodiesel has strong tendency to absorb water which might promote hydrolytic or hydrolytic oxidation [10,11]. The biodiesel will oxidize faster if there is oxygen and heat exists. The corrosion of the metal will faster due to the hydrolytic oxidation of biodiesel which increased the acidity of biodiesel. The corrosive nature of biodiesel can be more aggravated if free water and free fatty acid are present in it. Beside this, auto-oxidation of biodiesel can also enhance its corrosive characteristics and degradation of fuel properties[1].

There are only few studies available in the literature related to corrosion of different metals in biodiesel[10]. Most of these studies find corrosiveness of different biodiesel other than palm biodiesel. Kaul et al. investigated the corrosiveness of different biodiesels such asJatrophacurcas, Karanja, Mahua and Salvadora and compared withthe diesel fuel[12]. Further they found that biodiesel from Jatrophacurcas and Salvadora were more aggressive for both ferrous and non-ferrous metal. Geller et al. have reported that the ferrous alloys and copper alloys are more prone to be attracted by corrosion into fat based biodiesel[13].

METHODOLOGY

Aluminium Alloy (AA 5083) specimens were cut into 25mm×25mm×3mm coupons for immersion tests. Before exposure, the samples were mechanically polished using 600 to 1500 Silicone Carbide abrasive papers and lubricated using distilled water. The polished samples were cleaned with acetone, washed using distilled water, dried in air and stored over a desiccant[14,15].

The static immersion tests were carried out at 60^0C for 1632 hours (around 68 days). The Aluminium coupons were immersed into the beakers which containing the biodiesel and immersed the beaker into the oil bath. Felda brand's Saji cooking oil was used as oil bath heating oil.

A Nicolet™ 380 Fourier transform infrared (FT-IR)spectrometer equipped with standard KBr beam splitter and DTGS detector was used. The Smart ARK™ attenuated total reflection accessory was used to collect the data and the acetone was used for cleaning before background collection. The biodiesel and cooking oil samples were put in the FT-IR spectroscopy to analyse the percentage of the transimitter of the infrared which can pass through the samples. The data were collected using OMNIC™ spectroscopy software for further analysis.

Specimens were weighed for the original weight (w_0) and then hung in test solution for 68 days. The corroded specimens were then removed from the solutions, cleaned with distilled water and dried, then immersed in a nitric acid (HNO_3) for 2 to 3 min to remove the corrosion products. Finally, the coupons were washed with distilled water, dried and weighed again in order to obtain the final weight (w_1).

The weight loss of each test metal was recorded and the corrosion rate or penetration was calculated[4,16], according to the formulas given below:

$$\text{Corrosion Rate} = \frac{\text{Weight Loss X 534}}{(\text{Area})(\text{Time})(\text{Metal Density})} \text{ mils/ year or mpy}$$

$$\text{Penetration} = \frac{\text{Weight Loss X 372}}{(\text{Area})(\text{Time})} \text{ mg/ (sq.dm)(day) or mdd}$$

Where corrosion rate "mpy" stands for mils (0.001 inch) per year, weight loss in mg, density is in g/cm^3, exposed surface area in square inch and exposure time is in hours.

The Aluminium alloy (AA 5083) specimens for each concentration were immersed in a 100ml beaker containing seawater[14,15]. All the electrochemical measurements were obtained using Autolab Frequency Response Analyzer (FRA) coupled to an Autolabpotentiostat connected to a computer. The cell used comprised the conventional three electrodes with a platinum-wire counter electrode (CE) and a saturated calomel electrode (SCE) as reference, to which all the potentials were referred.

Aluminium alloy couponswere used as working electrode (WE). The electrode was polished mechanically and degreased by acetone. The exposed area to the test solution was 6.25 cm^2. The working electrode was first immersed in the test solution and after establishing a steady state open circuit potential, the electrochemical measurements were performed.

The potentiodynamic current–potential curves were recorded by changing the electrode potential automatically from -250 mV to +250 mV, related to the open circuit potential, with the scanning rate of 5 mV s^{-1}. Corrosion current densities (i_{corr}) and corrosion potential (E_{corr}) were evaluated from the intersection of the linear anodic and cathodic branches of the polarization curves as Tafel plots.

The Linear Polarization Resistance (LPR) measurements were carried out from -10 mV to +10 mVvsE_{corr} at scan rate of 1 mV s^{-1}. The impedance measurements were conducted over a frequency range of 5 x10^{-5} Hz down to 5 x 10^{-3} Hz. The results were analyzed using the fit program FRA.

RESULT AND DISCUSSION

Fourier transform infrared spectroscopy (FT-IR)

The peak of the wavenumber (cm^{-1}) of each functional group for the biodiesel samples were defined by using FT-IR. There have several main functional groups exist in the biodiesel which are mostly formed by the alcohol (CO stretching and OH stretching), lipid and protein (CH_3 Stretching and CH_2 Stretching), ester and etc.

From the graph, the ester has the higher peak at 1742.9 ±10 cm^{-1} (C=O stretch occurs in the range 1750-1735 cm^{-1}in normal esters)[11]. The conjugation in the acyl portion of the molecule moves the absorption to a lower frequency; conjugation with the O in the alkoxy portion moves the absorption to a higher frequency. Ring strain in cyclic esters (lactones) moves the absorption to a higher frequency. Beside this, the symmetric vibration of -C-H of CH_2 and CH_3 at 2854.4 ± 10 cm^{-1} and the asymmetric vibration of -C-H of CH_2 at the peak of 2924.1 ± 10 cm^{-1} were existing[11]. In addition, Alcohols (OH stretching) at the peak from range 3300- 3400 cm^{-1}and (CO stretching) at the peak from range 1000- 1200cm^{-1}.

The research also found out that the usual C=O stretching of the acid or the ester is replaced by two bands which arise from symmetrical and anti-symmetrical stretching vibrations of the COO- ion[16]. However, notable was the appearance of a broad band in the O-H stretching region (approximately at 3400 cm^{-1}) in the biodiesel samples. However the study of the IR spectra of highly unsaturated drying oils during autoxidation, the ester carboxyl band at 1740 cm^{-1} was seen to increase and widen, "indicating formation of compounds containing other C=O groups not completely resolved in their spectra from the ester carboxyl groups."

According to Maleque et al.[3], the palm oil contains 50-70 % of palmitic acid, $C_{15}H_{31}COOH$, which is a form of glycerine and it was an ingredients of much fat which can acts as a lubricating oil additives due to the presence of the long-chain fatty acid in vegetable oils. Early research also reported that the best boundaries additives use in lubricated contacts are log chain molecules with an active end group, typically organic alcohols, amines or fatty acid[8]. Therefore, we can conclude that the fatty acid of the POME composition can provide effective boundary lubrication due to the presence of a polar and this polar structure would form an effective boundary layer which dissipates non-polar molecules[2].

In previous study, the Curcas biodiesel has high concentration of C18:2 (19-41%) acid which is more prone to oxidation due to presence of two double bonds[17]. However, with all biodiesel samples the corrosion is within permissible limits. Therefore, even palm diesel prone to oxidation and increases of acidity but it might not corrode the metals due to its low concentration of C18:2 (10.1%).

The FT-IR graph for the pure biodiesel and FT-IR

FULL PAPER

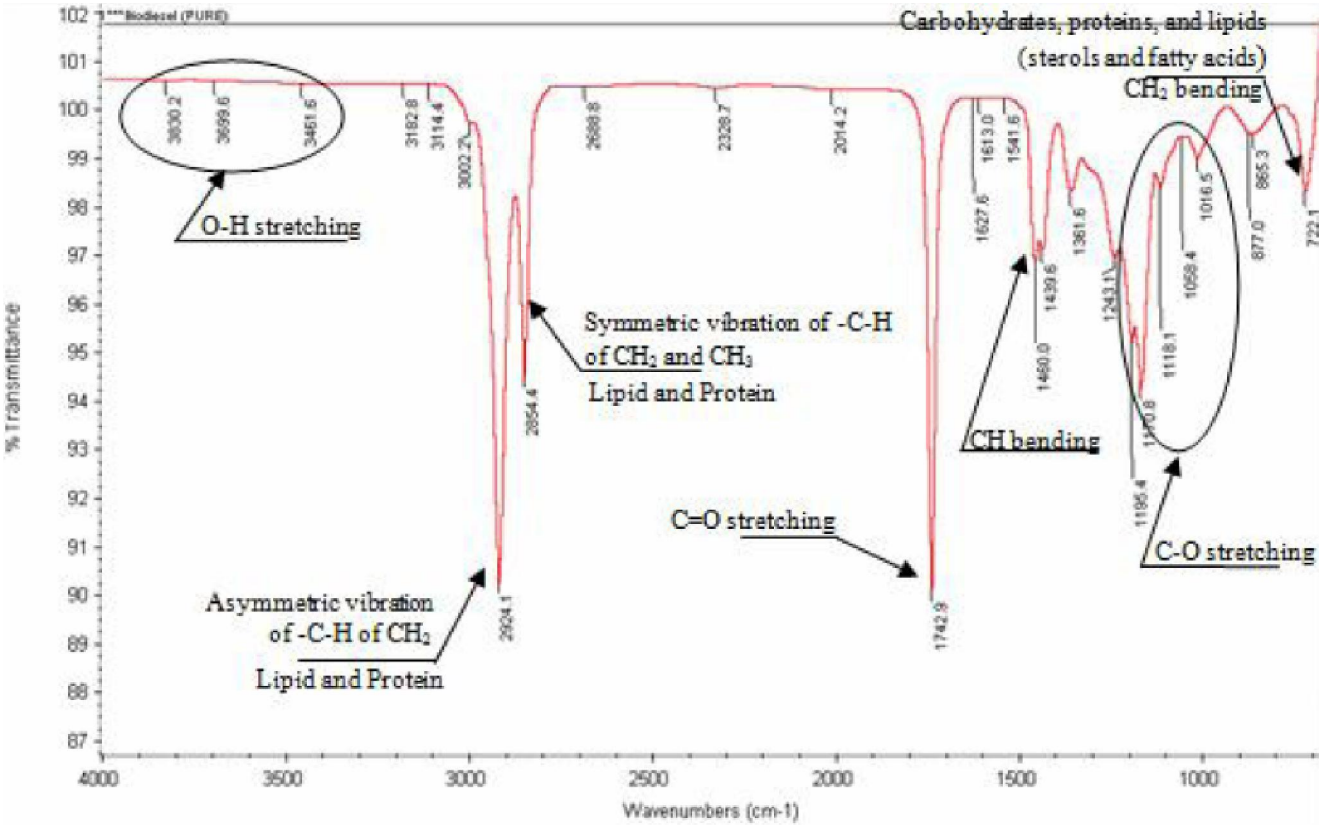

Figure 1: The FT-IR graph for pure biodiesel

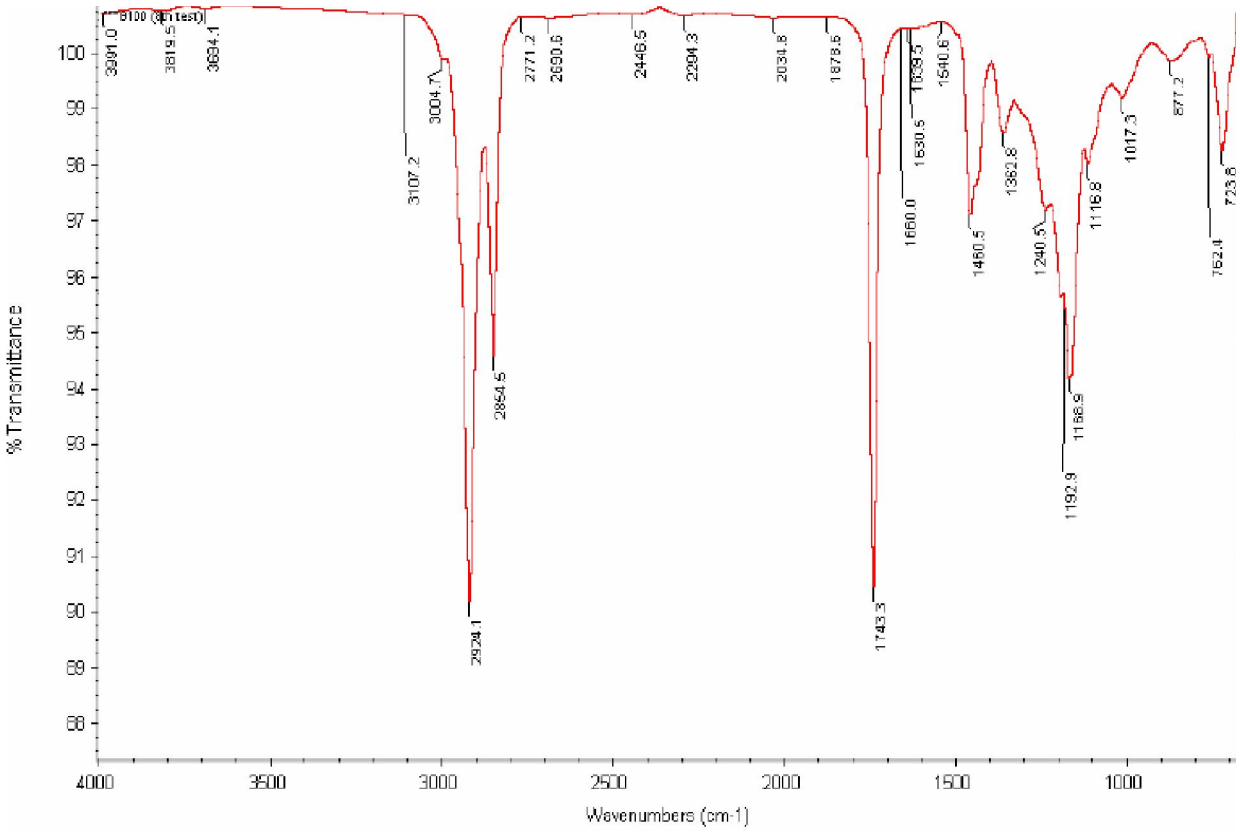

Figure 2 : The FT-IR graph for the 6th Test (Week 9)

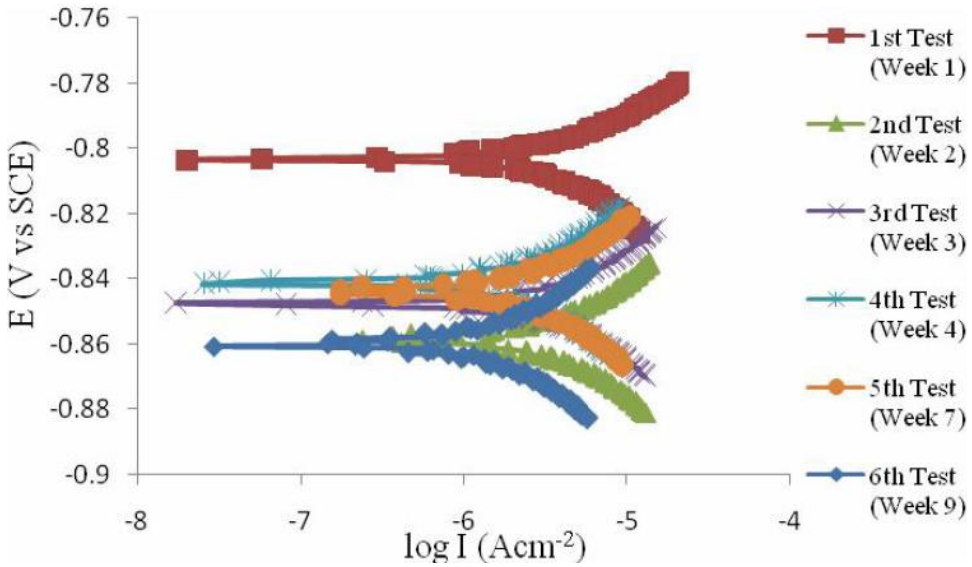

Figure 3 : Potentiodynamic polarization curve for the aluminium coupons from 1st Test (Week 1) to 6th Test (Week 9).

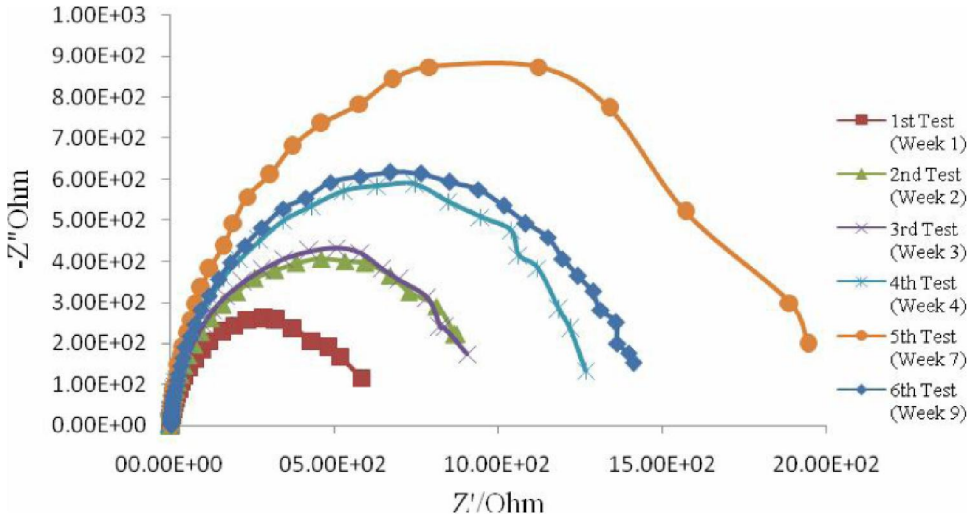

Figure 4 : Nyquist plot for the aluminium coupons from 1st Test (Week 1) to 6th Test (Week 9).

graph for 6th Test (Week 9) were shownbelow in the Figures 1 and 2 respectively.

Potentiodynamic polarization measurements

Figure 3 shows that the potential Voltage, E (V vs SCE) of the AA 5083 of each week which against the Current, I (Acm^{-2}). Potential voltage, E of AA 5083 was shifting from positive to negative direction from 1st week to 2nd week. But potential voltage, E of the 3rd week was decreased and shifting from negative to positive direction. At week 4, AA 5083 coupon was found out that the potential voltage, E was shifting to more positive direction but the E shifting back to negative direction on the 5th Test (Week 7) of the AA 5083 coupon during the test. Lastly, the potential voltage, E at week 7 was shifting to more negative direction compare to previous weeks.

From the potentiodynamic polarization curvethroughout the testing period1st Test (Week 1) to 6th Test (Week 9), we can see that the anodic and cathodic polarization curve of the AA 5083 alloy in the biodiesel. From the graph, we can see that the corrosion potential shift toward more negative direction and the anodic reaction control the rate of corrosion (as the anodic over voltage is higher). The Aluminium coupons were randomly taken out from the beakers for testing the corrosion rate. From the graph, we can see that the potential Voltage, E (V vs SCE) of the Aluminium which against the Current, I (Acm^{-2}) were shifting from positive to negative direction throughout the testing period

FULL PAPER

TABLE 1 : The electrochemical parameter of aluminium (AA 5083)

Test	Rp (kΩ)	E_{corr} (mV)	b_c (mV/dec^{-1})	b_a (mV/dec^{-1})	I_{corr} (μAcm^{-2})	C_{dl}
1st Test (Week 1)	2.91	-804	70	38	5.86	3.26E-04
2nd Test (Week 2)	3.90	-858	93	59	6.41	1.28E-04
3rd Test (Week 3)	0.60	-848	107	53	6.43	2.30E-04
4th Test (Week 4)	4.60	-841	131	66	6.63	1.01E-04
5th Test (Week 7)	0.71	-842	58	75	7.11	1.63E-04
6th Test (Week 9)	1.15	-859	55	58	1.06	6.19E-05

TABLE 2 : Weight loss measurement

Coupon	Before Immersion (in g)	After Immersion (in g)	Weight Loss (in g)	Average Weight Loss (in mg)	Corrosion Rate (mpy)	Corrosion rate (mmpy)	Remarks
1	4.5970	4.5968	0.0002	1.4500	2.2250	0.0565	1st Test (Week 1)
2	4.7116	4.7077	0.0039				
3	4.6857	4.6855	0.0002				
4	4.7151	4.7136	0.0015				
5	4.7096	4.7079	0.0017	2.8500	1.7319	0.0440	2nd Test (Week 2)
6	4.7240	4.7199	0.0041				
7	4.7317	4.7301	0.0016				
8	4.7323	4.7283	0.0040				
9	4.7475	4.7461	0.0014	1.2000	0.4553	0.0116	3rd Test (Week 3)
10	4.6995	4.6984	0.0011				
11	4.7488	4.7483	0.0005				
12	4.7214	4.7196	0.0018				
13	4.7354	4.7346	0.0008	1.3250	0.4194	0.0107	4th Test (Week 4)
14	4.7371	4.7357	0.0014				
15	4.574	4.5727	0.0013				
16	4.7173	4.7155	0.0018				
17	4.7072	4.7058	0.0014	1.0000	0.2395	0.0061	5th Test (Week 7)
18	4.7219	4.721	0.0009				
19	4.6715	4.6708	0.0007				
20	4.7305	4.7289	0.0008	0.8333	0.1496	0.0038	6th Test (Week 9)
21	4.6441	4.6424	0.0008				
22	4.7329	4.7312	0.0008				

but it shifting back on the 5th Test (Week 7) of the Aluminium coupon when taken for testing the corrosion rate and potentiodynamic polarization of the Aluminium.

When the potential voltage, E moves from positive to negative direction, it determines that the AA 5083 has higher resistance, R to reduce the corrosion. Therefore, the positive or negative direction of the potential voltage, E can be use to determine the resistance, R of the AA 5083. Higher resistance, R of AA 5083 can reduce the corrosion occur.

Electrochemical impendence spectroscopy (Nyquist plots)

Figure 4 shows that the electrochemical impendance spectrscopy (EIS) (Nyquist plot) of the Aluminium alloy throughout the testing period from 1st Test (Week 1) to 6th Test (Week 9). By analyzing the shape of the obtained Nyquist plots, it can be concluded that the curves approximated by a single capacitive semicircles, showing that the corrosion process was mainly charge transfer controlled and this might contributed the formation of oxide layer on aluminium coupons. The gen-

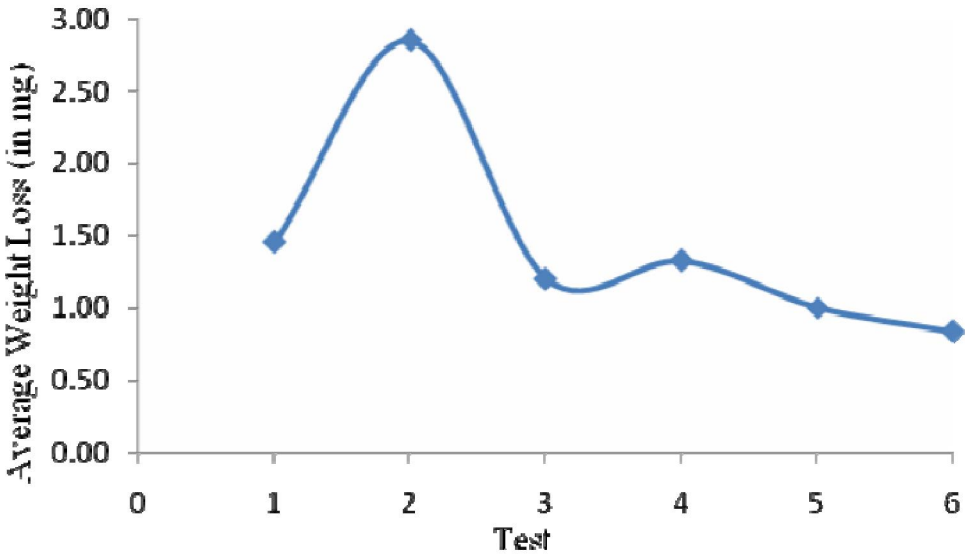

Figure 5 : Weight loss of AA 5083 coupons

eral shape of the curves can be observed to be very similar for all the samples and this is maintained throughout the whole test period, indicating that almost no change in the corrosion mechanism occurred due to the corrosion resistant addition.

Therefore, from the graph below (Figure 4), we can see that the lower or smaller of the semi-circle occur, the more corrosive of the aluminium is and the higher or larger of the semi-circle occur, the less corrosive of the aluminium. For the 1st Test (Week 1), the aluminium was more corrosive that the 2nd Test (Week 2) and the corrosion of the AA 5083 coupons had been inhibited due to the higher or larger of the semi-circle. The AA 5083 coupon has increased the size of the semi-circle from 2nd Test (Week 2) to 5th Test (Week 7) and AA 5083 become less corrosive each week compare with the previous weeks. But on th 6th Test (Week 9), the semi-circle started to become smaller and AA 5083 become corrosive. This is due to the breaking boundary of the oxide layer which formed on the aluminium coupons and this also means that the aluminium coupon now start to corrode products.

The corresponding corrosion potentials (E_{corr}), corrosion current density (I_{corr}), anodic Tafel slopes (b_a), cathodicTafel slopes (b_c), and corrosion rate (CR) were calculated and given bellow. The Polarization Resistance (Rp) shown that the higher value of the Rp is, the lower corrosion rate that might occur. The higher Rp which be recorded was on the 4th Test (Week 4), 4.6 k&!. The change in *E*corr is assumed to be related to the growth of a passive layer at the surface of electrode. From here we can see that the Ecorr for the 1st Test (Week 1) was -804mV and this valuewere increased afterward. After the 1st Test (Week 1), we can see that the Ecorr for the 2nd Test (Week 2) and the following tests, the Ecorr were constantly form the passive layer at the surface of electrode. The bc and ba also indicated that the biodiesel was the cathodic type of inhibitor at the 1st place and slowly to become mix type of inhibitor from 1st Test (Week 1) to 6th Test (Week 9). This is because the difference between the bc and ba (in mV/dec^{-1}) had slowly decreased.

The changes observed in the polarization curves after addition of the resistant are usually used as criteria to classify resistant as cathodic, anodic or mixed. The higher of the Polarization Resistance (Rp) value indicates the lower rate of corrosion[14,15]. The rate of cathodic reaction controls the rate of the corrosion process (as the cathodic over voltage is much greater than the anodic one[5,18]. The icorr (μAcm^{-2}) is increasing with the time of immersion from week 1 till week 6 but the icorr rapidly decrease on week 9 ($1.06\mu Acm^{-2}$) due to the breaking bond of the amine (-N-H-) of the biodiesel.

The values of polarization or charge-transfer resistance, R_{ct}, and double-layer capacitance, C_{dl}, for AA 5083 were presented in TABLE1. The values of R_{ct} are observed to increase with the increasing corrosion resistant concentration. It should be noted that while R_{ct} values increase with the addition of corrosion resistant, the C_{dl} values decrease indicating the formation of

a surface film. Thus, effective corrosion resistance is observed to be associated with high R_{ct} and low C_{dl} values. Increase in R_{ct} values and decrease in C_{dl} values was related to the increased degree of protection of AA 5083 alloy in seawater.

The TABLE 1 shows that the C_{dl} values were increased while the R_{ct} values were decreased. The higher value of the C_{dl} was 3.26E+04 on the 1st Test (Week 1) while the R_{ct} was 2.91k&! and the lower value of $C_{dl}$was 6.19E+05 on the 6th Test (Week 9) while the R_{ct}was1.15kΩ .

Weight loss measurement

TABLE 2 shows the weight loss measurements of the aluminium coupons from time to time. From here, we can see that there is no much difference in weight (in g) of the aluminium coupons before immersion and after immersion throughout the test period but the corrosion rate of AA 5083 having some changing from Week 1 to Week 9.

The weight loss of AA 5083 is shown in Figure 5. From the graph, we can see that the weight loss was decreased with increased the immersion time. The highest weight loss was recorded as 2.85 mg on 2nd Test and decreased after the 2nd Test. The lowest weight loss value was recorded on 6th Test as low as 0.83 mg.

Although the average weight loss of AA 5083 were not significant but this will affect the corrosion rate of the AA 5083 throughout the testing period. For the corrosion rate of the AA 5083, we can see that there have some decreased of the corrosion rate from time to time. The corrosion rate of the 1st Test (Week 1) was 2.2250 mpy and decreased to 0.1496 mpy on 6th Test (Week 9). But there has the dramatic decreased of corrosion rate between 2nd Test and 3rd Test. The corrosion rate for 2nd Test was 1.7319 mpy and rapidly decreased to 0.4553 mpy for 3rd Test.

CONCLUSION

The existing of fatty acid in the POME composition, this can provide an effective boundary layer (boundary lubrication) due to the presence of polar structure which dissipates non-polar molecules or corrosion inhibitor. Aluminium also forms an oxide film when contact with the biodiesel. The oxide film also can give certain of rate of protection to the aluminium and to prevent the corrosion. Aluminium is able to resist the corrosion due to its phenomenon of passivation. Therefore use of Electrochemical Impendence Spectroscopy (EIS) measurements only clarified that the corrosion process was mainly charge-transfer controlled and no change in the corrosion mechanism occurred either due to the immersion time or to the inhibitor addition to acidic solutions.

Although the acidity of the biodiesel will increased due to the immersion period but there has only slightly change on its properties. The higher peak of the wavenumber for CH_2 and C=O stretching were almost constant (2923$cm^{-1}$to 2924 cm^{-1}) throughout test period. Beside this, there was no water content occur in the biodiesel during the test due to the no change of the peak of wavenumber for the OH stretching.

For the weight loss measurement, there only a slightly change of the weight loss between the AA 5083 sample before immersion and after immersion but there was a decreased of the corrosion rate of AA 5083 from 1st Test (2.2250 mpy) to 6th Test (0.1496 mpy). As the immersion time increased, the value of Rp also increased and decreased throughout the test period. The highest value of Rp is at 4th Test (Week 4), 4.6 k&! while the C_{dl} is recorded at 1.01E-04 and it was the second lowest value throughout the test period. The result of the 4th Test also shows that the value of I_{corr}, b_a, b_c and E_{corr} were -841mV, 131 mV/dec^{-1}, 66 mV/dec^{-1} and 6.63 μAcm^{-2}respectively.

REFERENCES

[1] Jon Van Gerpen; Biodiesel processing and production. Journal of Fuel Processing Technology, **86**, 1097– 1107 **(2005)**.

[2] M.A.Kalam, H.H.Masjuki; Recent Development on Biodiesel in Malaysia. Journal of Scientific & Industrial Research, **64**, 920-927 **(2005)**.

[3] M.A.Maleque, H.H.Masjuki, S.M.Sapuan; Vegetable-based biodegradable lubricating oil additives.Journal of Industrial Lubrication and Tribology, **55(3)**, 137-143 **(2003)**.

[4] M.Canakci, H.Sanli; Biodiesel production from various feedstocks and their effects on the fuel properties.Journalof Industrial Microbiology Biotechnology, **35**, 431–441 **(2008)**.

[5] Palligarnai Vasudevan, Boyi Fu. Environmentally Sustainable Biofuels: Advances in Biodiesel Research. Waste Biomass Valor, **1**, 47-63 **(2010)**.

[6] S.Sukkasi, U.Sahapatsombut, C.Sukjamsri, S.Saenapitak, Y.Boonyongmaneerat; Electroless Ni-based coatings for biodiesel containers. Journal of Coating Technology and Research, **8(1)**, 141-147 **(2010)**.

[7] Karavalakis, Stamoulis, Stournas, Dimitrios Karonis; Evaluation of the oxidation stability of diesel/ biodiesel blends. Fuel, **89**, 2483-2489 **(2010)**.

[8] Rosen Dinkov, GeorgiHristov, DichoStratiev, VioletaBoynova Aldayri; Effect of commercially available antioxidants over biodiesel/ diesel blends stability. Fuel, **88**, 732-737 **(2009)**.

[9] W.B.Wan Nik; Performance Investigation of Energy Transport Media as Influenced by Crop Based Properties, UTM/RMC/F/0014, **(1998)**.

[10] A.S.M.A.Haseeb, S.Y.Sia, M.A.Fazal, H.H.Masjuki; Effect of temperature on tribological properties of palm biodiesel. Journal of Energy, **35**, 1460–1464 **(2010)**.

[11] G.Kenothe; Analyzing Biodiesel: Standard and Other Methods. Journal of American Oil Chemist's Society, **83**, 823-833 **(2006)**.

[12] S.Kaul, R.C.Saxena, A.Kumar, M.S.Negi, A.K.Bhatnagar; Corrosion behavior of biodiesel from seed oils of Indian origin on diesel engine parts.Journal of Fuel Process Technology, **88**, 303–307 **(2007)**.

[13] D.P.Geller, T.T.Adams, J.W.Goodrum, J.Pendergrass; Storage stability of poultry fat and diesel fuel mixtures: specific gravity and viscosity. Fuel, **87**, 92–102 **(2008)**.

[14] R.Rosliza, W.B.Wan Nik, S.Izman, Y.Prawoto; Anti-corrosive properties of natural honey on Al–Mg–Si alloy in seawater. Journal of Current Applied Physics, **10**, 923–929 **(2010)**.

[15] R.Rosliza, Wan W.B.Nik, H.B.Senin; Electrochemical properties and corrosion inhibition of AA6061 in tropical seawater. Colloids and Surfaces A: Physicochem. Engineering Aspects, **312**, 185–189 **(2007)**.

[16] Leon G.Schumacher, Nancy Elser; Sample Analysis from Biodiesel Test, Agricultural Engineering Department, University of Missouri-Columbia, **(1997)**.

[17] G.S.Dodos, F.Zannikos, S.Stournas; Effect of metals in the oxidation stability and lubricity of biodiesel fuel, SAE Technical Paper No., 2009-01-1829 **(2009)**.

[18] M.A.Moharam, L.M.Abbas; A study on the effect of microwave heating on the properties of edible oils using FTIR spectroscopy. African Journal of Microbiology Research, **4(19)**, 1921-1927 **(2010)**.

[19] J.A.Williams; Engineering Tribology, Oxford University Press, Oxford, UK, 166-168 and 358-58 **(1998)**.